The static detailed structure and dynamical behaviours of molten copper halides

1997 J. Phys.: Condens. Matter 9 10101

(http://iopscience.iop.org/0953-8984/9/46/008)

J. Phys.: Condens. Matter **9** (1997) 10101–10113. Printed in the UK PII: S0953-8984(97)83991-4

The static detailed structure and dynamical behaviours of molten copper halides

T Koishi†, Y Shirakawa‡ and S Tamaki§

† Graduate School of Science and Technology, Niigata University, Niigata 950-21, Japan
‡ Department of Materials Science and Processing, Faculty of Engineering, Osaka University, Osaka 565, Japan
§ Department of Physics, Faculty of Science, Niigata University, Niigata 950-21, Japan

Received 7 May 1997, in final form 1 July 1997

Abstract. By using well-established pairwise potentials in which a partially covalent bonding character is taken into account, detailed structural properties and the diffusion constants for molten CuCl, CuBr, and CuI have been simulated. The results obtained from the velocity correlation function method and those obtained from the mean square displacement one agree well. The activation energies for cations and anions are discussed in connection with the local ionic configuration. The shear viscosities for these molten salts at various temperatures are also estimated by using a nonequilibrium molecular dynamics simulation. The results for CuCl are fair to good in comparison with experimental data.

1. Introduction

There is a long-established procedure for deriving static structure factors of molten salts that is based on the use of x-ray and neutron diffractions. A detailed review article on this subject by Revere and Tosi has appeared [1]. In particular, the success of the separation of the partial structure factors of molten salts by using the techniques of isotope enrichment via neutron diffraction [2, 3] and anomalous x-ray scattering [4] has led to some useful information on their detailed configurations becoming available.

For some time, the bonding nature of liquid copper chlorine has been controversial: is it of molecular type or ionic? Page and Mika measured the structure of molten CuCl by means of neutron diffraction [5], and later a more detailed study which involved deriving the three partial structure factors was carried out for this molten salt by Eisenberg *et al* [6]. According to their results, the partial pair correlation function $g_{\mathrm{CuCu}}(r)$ is quite different from the usual pair distribution functions of simple liquids such as alkali metals: it has a broadened first peak, and its oscillation is also obscure—it is as if the Cu^+ ions distribute randomly—and it has no detailed structure. This type of total structure factor has often been seen for molecular liquids; Powles [7] explained it using a model of the formation of CuCl molecules. However, this model was criticized by Gillan [8], and, furthermore, Boyce and Mikkelsen [9] demonstrated that molten CuCl is composed of Cu^+ and Cl^- ions, by means of measurements of the nuclear relaxation times for Cu and Cl atoms in it.

The problem is that of explaining why the structure of molten CuCl indicates such a type of molecular liquid behaviour. The answer to this may be that this is due to molten CuCl having partially covalent bonding. In fact, this idea has been adopted by several workers [10], and recently Stafford *et al* [11] proposed effective pair potentials for molten

0953-8984/97/4610101+13$19.50

copper halides (CuCl, CuBr, and CuI) in which they took a partial covalency into account by having an effective charge less than unity in their Coulomb interaction potentials. By using these potentials and molecular dynamics (MD) simulation, they derived the partial pair correlation functions for molten copper halides, and the results are in fairly good agreement with experimental ones. It should be emphasized that the effective charges of these halides are somewhat smaller than unity, indicating a coexistence of partially covalent bonding.

In this paper, we will report more detailed information on the detailed structures and the dynamical properties, such as the viscosity and the diffusion constant, for molten copper halides obtained by using the same potentials as were proposed by Stafford *et al* [11]. Also, for comparison, the results on the detailed structure of molten NaCl obtained by using the well-established Tosi–Fumi [12] potentials will also be presented.

2. The computer simulation method

The interactions between the ions in molten copper halides are essentially as given by Vashishta and Rahman [13]:

$$\phi_{ij}(r) = \frac{A(\sigma_i + \sigma_j)^n}{r^n} + \frac{z_i z_j e^2}{r} + \frac{1}{2}\frac{\alpha_i z_j^2 + \alpha_j z_i^2}{r^4} - \frac{C_{ij}}{r^6} \tag{1}$$

where A is a constant whose value is governed by the magnitude of the repulsion, σ_{ij} is the ionic radius, and $z_{i\,\mathrm{or}\,j}$ is the effective charge. To proceed with the simulation, the simpler formulae given below are used—that is, the van der Waals potentials between (i) positive and positive and (ii) positive and negative ions are neglected, and the positive-ion–positive-ion and positive-ion–negative-ion dipole–dipole interactions are also ignored, because the polarizability of negative ions is much larger than that of positive ions.

Table 1. The parameters of equation (2).

	CuCl	CuBr	CuI
n	7	7	7
H_{MM}	0.00389	0.00536	0.01196
H_{XX}	132.614	185.463	339.578
H_{MX}	4.292	5.986	12.982
$\lvert z\rvert$	0.501	0.4828	0.6
α_{X}	3.45	4.47	6.52
C_{XX}	5.773	9.028	6.93

Thus, the formulae for the pair potentials in molten copper halides used in practice in the simulations are as follows:

$$\begin{aligned}
\phi_{\mathrm{MM}}(r) &= \frac{H_{\mathrm{MM}}}{r^n} + \frac{z^2e^2}{r} \\
\phi_{\mathrm{XX}}(r) &= \frac{H_{\mathrm{XX}}}{r^n} + \frac{z^2e^2}{r} - \frac{\alpha_{\mathrm{X}}}{r^4} - \frac{C_{\mathrm{XX}}}{r^6} \\
\phi_{\mathrm{MX}}(r) &= \frac{H_{\mathrm{MX}}}{r^n} + \frac{z^2e^2}{r} - \frac{1}{2}\frac{\alpha_{\mathrm{X}}}{r^4}
\end{aligned} \tag{2}$$

where $z = |z_{\mathrm{M}}| = |z_{\mathrm{X}}|$. As seen in table 1, the effective charges $z_{i\,\mathrm{or}\,j}$ are taken to be 0.5 to 0.6, which indicates that the quantity $1 - z_{i\,\mathrm{or}\,j}$ is equal to the contribution of the covalency effect. It seems that the charge transfers from copper atoms to halogen ones are not entirely

complete, and the outer electron's configuration is, for each ion, fairly deformable by the configurations of the surrounding ions, and the effective charges contributing to the Coulomb interaction potentials in these systems should be, consequently, smaller than unity. In other words, there appears to be an increase in the degree of covalency of the bonding; otherwise the bonding energy due to just these Coulomb potentials would become smaller. However, it is emphasized that such covalency of the bonds is assumed to be independent of the structure. Although all of the relevant parameters are given by Stafford *et al* [11], they are also listed in table 1 for reference.

The molar volumes (cm^3 mol^{-1}) of molten CuCl, CuBr, and CuI used here are equal to the experimental values, and are expressed in the following forms [14]:

$$\text{CuCl:} \qquad V = 24.34(1 + 2.10 \times 10^{-4}T + 3.24 \times 10^{-8}T^2)$$
$$\text{CuBr:} \qquad V = 28.24(1 + 3.35 \times 10^{-4}T - 0.841 \times 10^{-8}T^2)$$
$$\text{CuI:} \qquad V = 34.71(1 + 3.83 \times 10^{-4}T - 5.12 \times 10^{-8}T^2).$$

Table 2. The parameters of equation (3).

	A (10^{-19} J)	B (Å^{-1})	$\sigma_i + \sigma_j$ (Å)	C (10^{-79} J m^6)	D (10^{-99} J m^8)
++	0.4225	3.15	2.34	1.68	0.80
+−	0.3380	3.15	2.75	11.20	13.90
−−	0.2535	3.15	3.17	116.00	233.00

The pair potentials for molten NaCl are given in the following forms:

$$\phi_{ij}(r) = \frac{z_i z_j e^2}{r} + A_{ij}\exp[B(\sigma_i + \sigma_j - r)] - \frac{C_{ij}}{r^6} - \frac{D_{ij}}{r^8} \qquad (z_i = z_j = 1). \tag{3}$$

The first term represents the Coulomb interaction, the second one represents the overlap repulsion, and the third and fourth terms represent the dipole–dipole and dipole–quadrupole dispersion forces. The values used for the various parameters in the potential (3) are listed in table 2.

The densities ρ (g cm^{-3}) used for molten NaCl are given experimentally by the form [15]

$$\rho = 2.1393 - 0.5430 \times 10^{-3}T. \tag{4}$$

We have carried out simulations for a system containing 512 ions with periodic boundary conditions, in deriving the pair correlation functions and other quantities. The integration of the equations of motion was performed via the algorithm developed by Verlet [16]. Starting from a random configuration, the procedure was carried out in 3000 time steps each of 3.0×10^{-15} s. The Ewald method was used for the summation of the Coulomb interactions in order to achieve better convergence.

3. Partial structure factors and local configurations

Initially, we re-examined the derivation of the partial structure factors of molten copper halides, and the results agree with the report by Stafford *et al* [11]. It is worth mentioning that there is an especially notable broadening of the first peak in the $g_{+-}(r)$s, which might be caused by smaller charges of ions, and that the present results for $g_{+-}(r)$ for molten CuCl agree with those obtained experimentally by Eisenberg *et al* [6].

Several interesting facts have, however, been established in addition to those described above. First, the probability of finding other ions at the distance r from an arbitrary ion

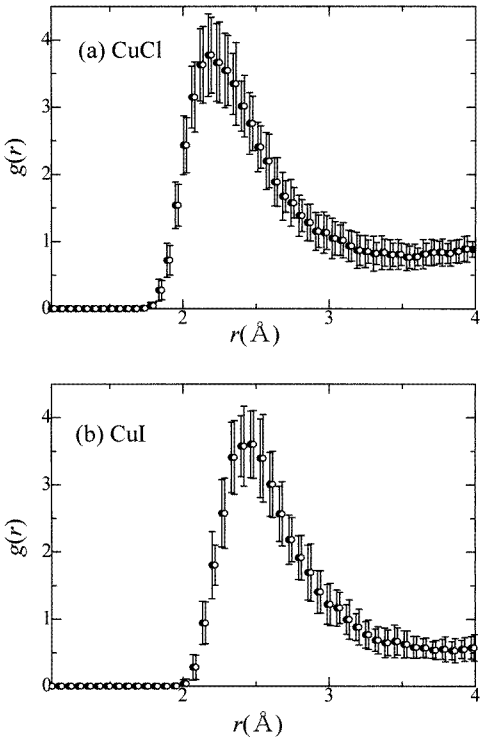

Figure 1. (a), (b) Pair distribution functions of oppositely charged ions i and j ($i, j = +, -$), $g_{ij}(r)$. Circles and solid circles are artificially separated for convenience; ○: anion distributions as 'seen' by cations; ●: cation distributions as 'seen' by anions; ⌶ and ⧳: the extent of the fluctuations in all of the pair distribution probabilities.

is not uniquely determined—that is, a local pair distribution at a given distance exhibits fluctuation to some extent and depends on the ions being centred. Examples are the cases of local distributions for molten CuI and CuCl, as seen in figures 1(a) and 1(b), although it is emphasized that the averaged values, described by $g_{+-}(r)$ (negative ions 'seen' from positive ions) and $g_{-+}(r)$ (positive ions 'seen' from negative ions), are completely equal to each other. The fluctuation for $g_{-+}(r)$ is somewhat bigger than that of $g_{+-}(r)$ at the position around that of the first peak.

It is, however, impossible to derive this interesting result by means of an ordinal diffraction experiment, because the experimental partial distribution function $g_{ij}(r)$ is only derived from the Fourier transform of the observed partial structure factor $S_{ij}(q)$ which is automatically equal to an averaged quantity. One possible experiment in which one might see such an effect obtained by computer simulation would be an EXAFS investigation using a strong photon source.

The second interesting fact is that the configuration of neighbouring negative ions around positive ions, called [nnn] (=number of nearest neighbours) in the following, shows a fluctuation:

$$[\text{nnn}] \equiv \int_0^{r_1} g_{ij}(r)\, 4\pi r^2 \, \mathrm{d}r \tag{5}$$

where r_1 is the position at which the extrapolation of the first peak of the curve $g_{ij}(r)\, 4\pi r^2$,

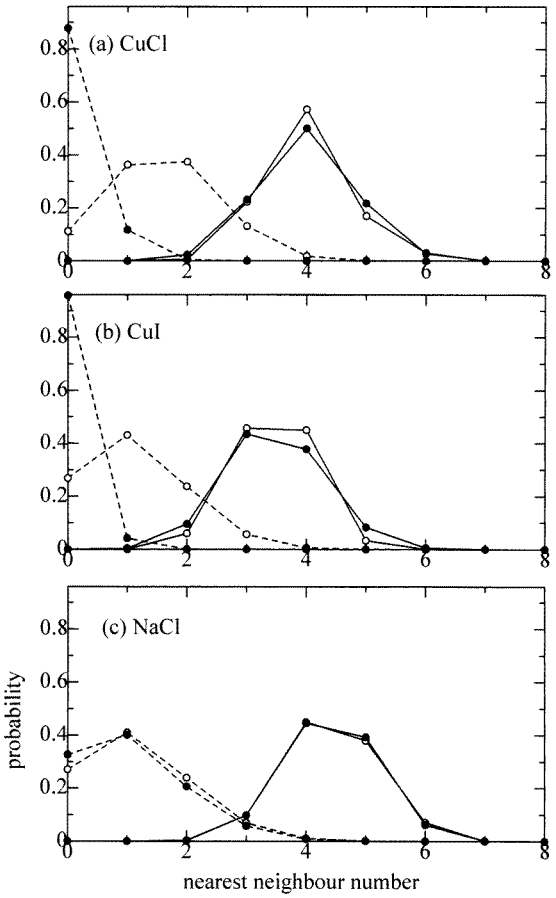

Figure 2. (a), (b) Distribution probabilities for molten CuCl and CuI with different and the same kinds of ion around the cations and anions, respectively, as functions of the number of nearest neighbours defined by equation (5): –○–: the anion distribution 'seen' by cations; –●–: the cation distribution 'seen' by anions; - -○- -: the cation distribution 'seen' by cations; - -●- -: the anion distribution 'seen' by anions. (c) Distribution probabilities for molten NaCl with different and the same kinds of ion around the cations and anions, respectively, as functions of the number of nearest neighbours defined by equation (5): –○–: the anion distribution 'seen' by cations; –●–: the cation distribution 'seen' by anions; - -○- -: the cation distribution 'seen' by cations; - -●- -: the anion distribution 'seen' by anions.

which is approximately a quadratic function, becomes zero. That of neighbouring positive ions around negative ions also ranges from two to five nearest neighbours, and the most probable configuration is three nearest neighbours, as shown in figures 2(a) and 2(b). For reference, the distribution of the number of nearest neighbours for molten NaCl is also shown, in figure 2(c). The average probabilities, arranged so as to have their zero points for the maximum value of [nnn] at the nearest-neighbouring site, are normalized to unity. The probability at the zero coordinate in these figures represents the probability of finding the same kind of ion having a zero coordinate. In other words, for example, the probability of finding an anion with the zero coordinate means that the probability of finding any other anions around the centred anion is equal to zero.

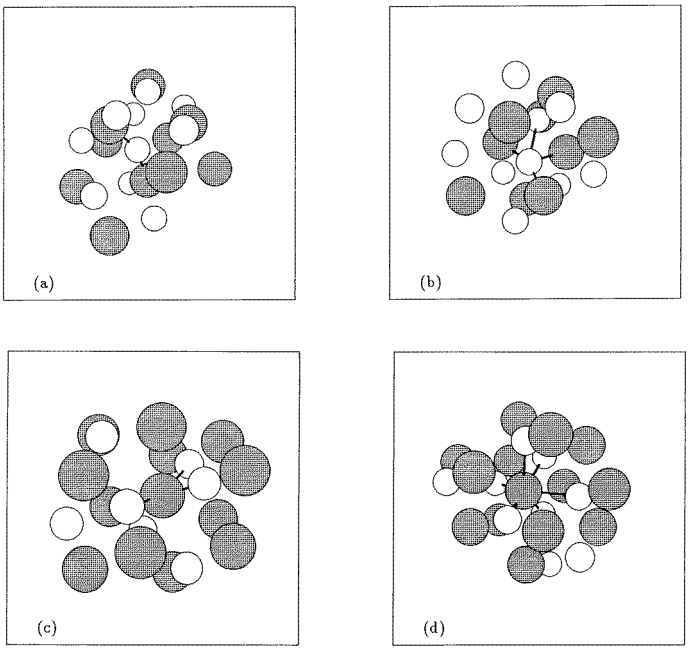

Figure 3. A typical snapshot of local structure in molten CuCl.

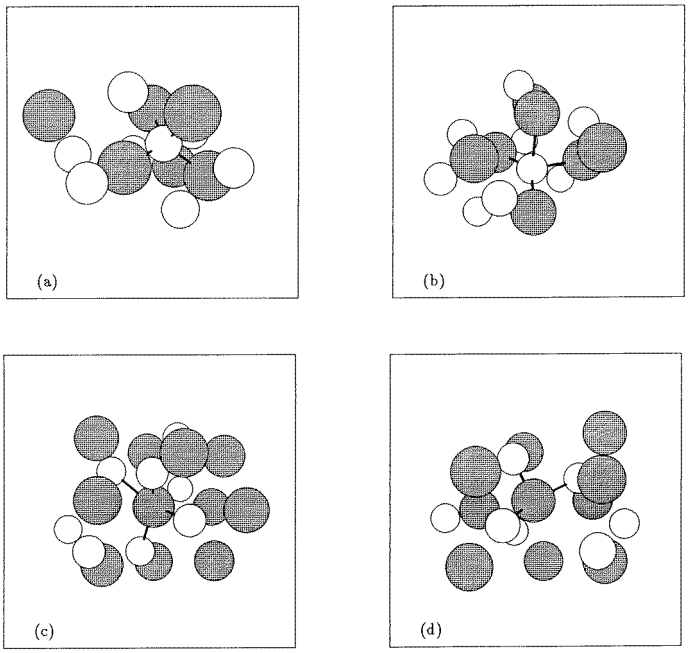

Figure 4. A typical snapshot of local structure in molten CuBr.

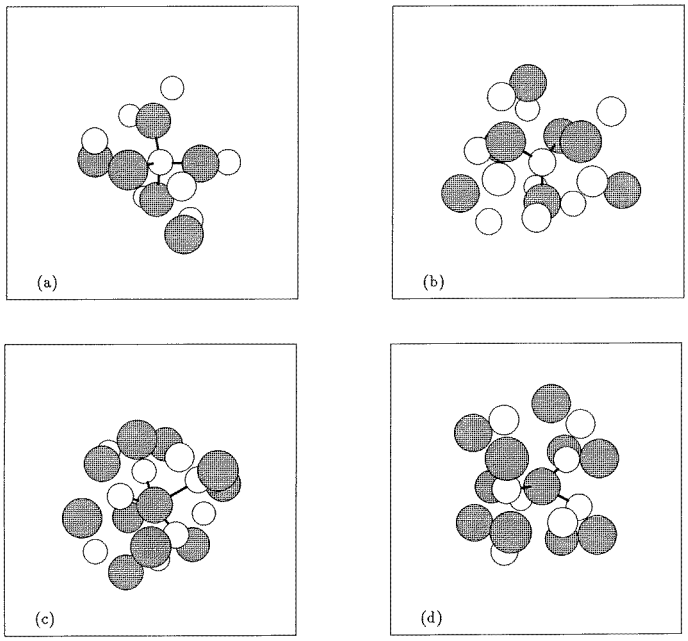

Figure 5. A typical snapshot of local structure in molten CuI.

There is some possibility of finding the same kind of ion in the nearest-neighbouring region. This tendency can be seen even for molten NaCl, in which the probability of the same kind of ion's location is about 0.2 to 0.3 for both positive and negative ions, as shown in figure 2(c). However, this tendency is more remarkable in the cases of molten copper halides, as shown in figures 2(a) and 2(b), although there is a small possibility of negative ions around any negative ions that are centred.

We present several snapshots of the spatial configurations for these molten salts. A typical snapshot of the local structure for molten CuCl is shown in figure 3. In this figure, the open circles indicate cations and the cross-hatched circles indicate anions. The second-nearest-neighbour ions of a centred ion are drawn and the lines to nearest-neighbour ions from the central ion are also shown. Figures 3 to 5(a) and 5(b) are snapshots 'seen' by a cation, and (c) and (d) are as 'seen' by an anion. These snapshots may correspond to the above interesting facts.

4. Temperature dependences of diffusion constants and shear viscosities

We have obtained the temperature dependences of the diffusion constants for molten copper halides by using the same potentials as were proposed by Stafford *et al* [11] and the MD simulation method. Furthermore, the shear viscosities of these halides have also been estimated, by using the nonequilibrium molecular dynamics (NEMD) simulation method proposed by Lees and Edwards [17]. In principle, the shear viscosity is obtainable by using the method of Green–Kubo correlation functions at thermal equilibrium [18]. However, this method is not always good enough if the number of particles in the simulation is less than 10^4. Compared with the Green–Kubo method, the above NEMD one is more accurate and powerful for deriving the shear viscosity [19].

The diffusion constants can be computed by two different ways. One is via the mean square displacement, $r^2(t)$, and the other is via the velocity correlation function, $f(t)$. The former is computed from the positions of the particles, $r_i(t)$, as follows:

$$r^2(t) = \frac{1}{N}\left\langle \sum_{i=1}^{N} |r_i(0) - r_i(t)|^2 \right\rangle \tag{6}$$

which, if t is large enough, is related to the self-diffusion constant:

$$D_M = \lim_{t\to\infty} \frac{1}{6t} r^2(t). \tag{7}$$

If t is small enough, we can write $\boldsymbol{r}(t_0 + t) - \boldsymbol{r}(t_0) \cong \boldsymbol{v}(t_0)t$, and

$$r^2(t) \cong \langle \boldsymbol{v}(0) \cdot \boldsymbol{v}(0) \rangle t^2 = \frac{3k_B T}{m} t^2. \tag{8}$$

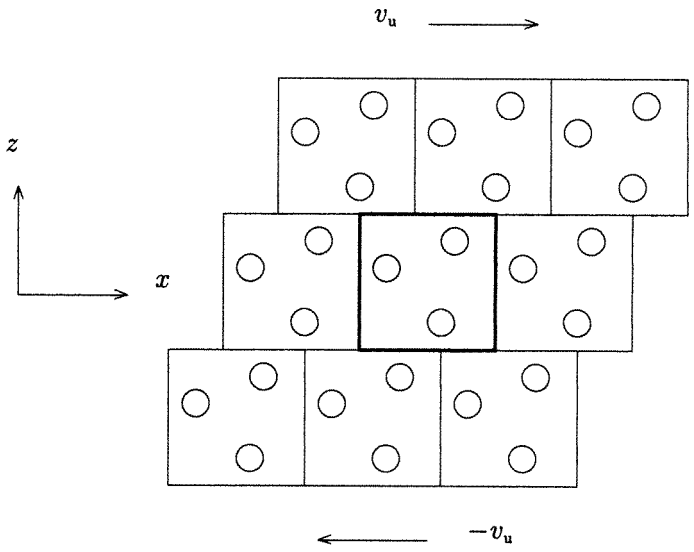

Figure 6. Boundary conditions used in deriving the viscosity by the NEMD method.

The velocity correlation function is computed from the velocities of the particles $\boldsymbol{v}_i(t)$ in terms of

$$f(t) = \left\langle \sum_{i=1}^{N} (\boldsymbol{v}_i(0) \cdot \boldsymbol{v}_i(t)) \right\rangle \tag{9}$$

and then the self-diffusion coefficient can be obtained from this function through the well-known formula [20]

$$D_V = \frac{k_B T}{m} \int_0^\infty (f(t)/f(0))\, \mathrm{d}t \tag{10}$$

where m is the mass of a particle.

The simulation for the NEMD method follows the work of Lees and Edwards [17], and was carried out for a system of 256 ions in 20 000 steps. During the course of the simulation, we artificially kept the temperature of the system fairly constant by scaling the velocities of all of the particles every 50 steps; thus the fluctuation of the temperature was

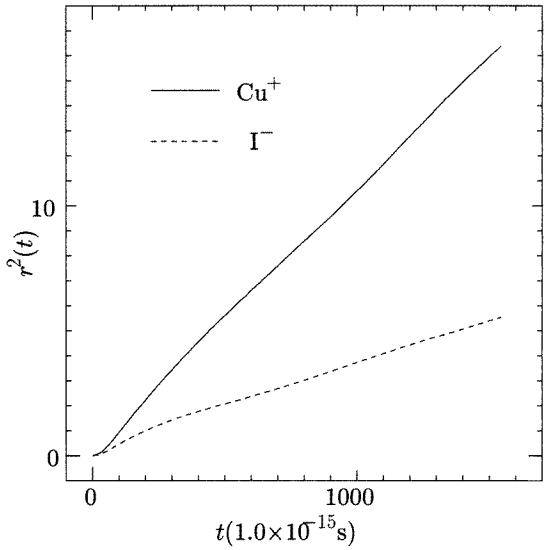

Figure 7. The mean square displacement function for molten CuI.

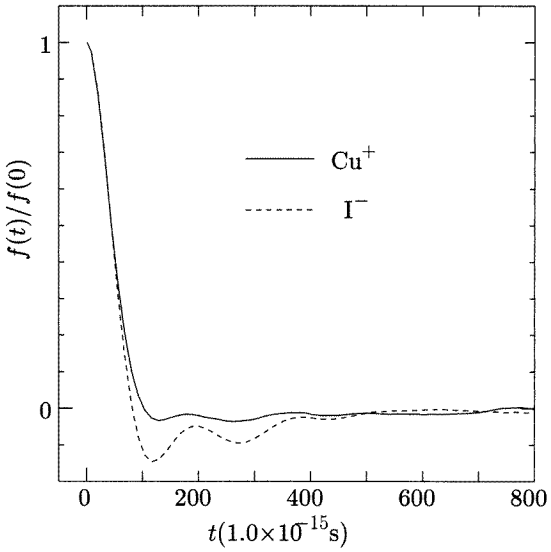

Figure 8. The normalized velocity autocorrelation function for molten CuI.

kept below 10 K. In the NEMD method for obtaining the shear viscosity, a time-dependent arrangement of replicas is used. The replica arrays are displaced in a special manner in order to create a Couette flow in the unit cell, as shown in figure 6. In the simulation cell, we have a velocity gradient $\partial u_x/\partial z$. The shear viscosity η is derived as follows:

$$P_{xz} = \eta \frac{\partial u_x}{\partial z} \tag{11}$$

where P_{xz} is the pressure tensor, and the shear viscosity η obtained from equation (11) depends on the velocity gradient. It is fairly well known [21] that the dynamical viscosity $\eta(\omega)$, where ω is equal to $\partial u_x/\partial z$, is proportional to $\omega^{1/2}$; that is,

$$\eta(\omega) = \eta_0 - A\omega^{1/2}. \tag{12}$$

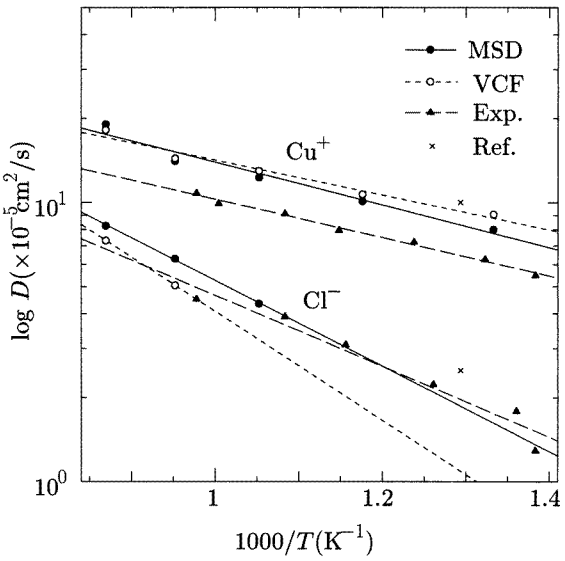

Figure 9. The temperature dependence of the diffusion constants for molten CuCl. 'Ref.' is taken from reference [22].

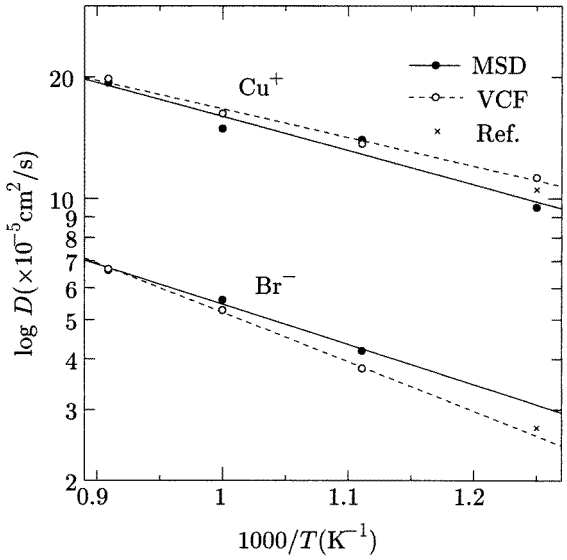

Figure 10. The temperature dependence of the diffusion constants for molten CuBr. 'Ref.' is taken from reference [22].

It is, therefore, usual for the viscosity, $\eta(0) = \eta_0$, to be derived by means of an extrapolation of the ω-dependence for $\eta(\omega)$. The results will be given in the following section.

5. Results

In figure 7 we show the mean square displacement (MSD) for molten CuI obtained by simulation. It is clear that the MSD is proportional to t at large t and to t^2 at small t. The slope of the proportionality to t gives the self-diffusion constant.

The normalized velocity correlation functions (VCFs) of molten CuI are shown in figure 8. As is seen in this figure, the VCF is close to zero at large t. By using this

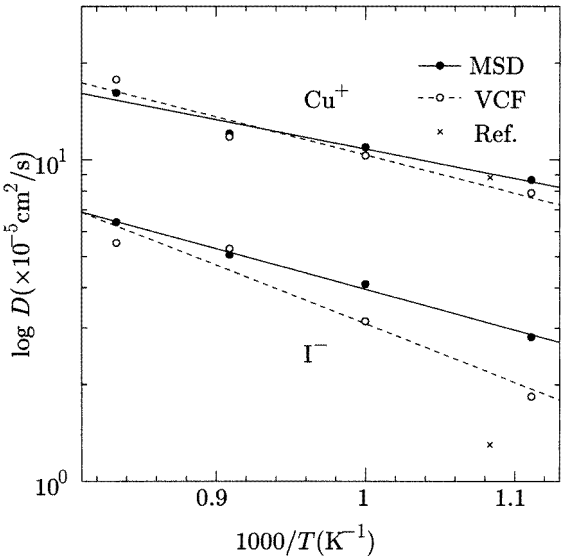

Figure 11. The temperature dependence of the diffusion constants for molten CuI. 'Ref.' is taken from reference [22].

function and equation (10), the diffusion constants at corresponding temperatures have also been obtained.

The temperature dependences of the diffusion constants for molten CuCl, CuBr, and CuI were obtained as shown in figures 9, 10, and 11 respectively. Some of results agree with those obtained by Trullàs *et al* [22], although the latter authors carried out their simulation for only one temperature for each system. According to these figures, the results for the diffusion constant obtained from the MSD method and the VCF method agreed well. In the low-temperature region, however, the VCF method is not satisfactory for deriving the diffusion constant, because the integrand in equation (10) does not converge to zero even for the present timescale of simulation.

Table 3. Values of D_0 and Q.

		D_0 (10^{-4} cm^2 s^{-1})	Q (10^4 J mol^{-1})
CuCl	D_+	8.10	1.46
	D_-	17.9	2.93
CuBr	D_+	11.1	1.61
	D_-	8.70	1.91
CuI	D_+	7.28	2.24
	D_-	8.80	2.28

In figures 12 and 13 we show the viscosity of molten CuCl, CuBr, and CuI estimated by using the NEMD method. For molten CuCl, the simulated result is close to the two sets of experimental data, although we are not sure which experiment is more accurate.

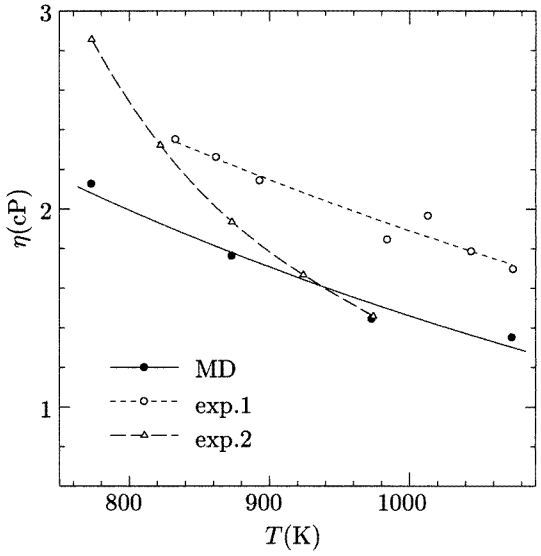

Figure 12. The temperature dependence of the viscosity for molten CuCl. 'exp.1' is taken from reference [24] and 'exp.2' is taken from reference [15].

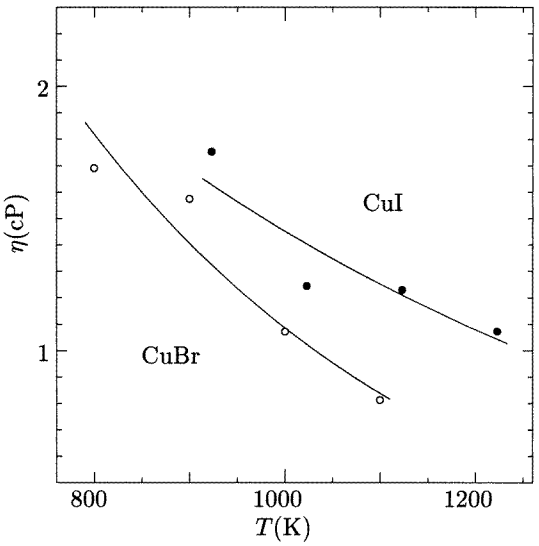

Figure 13. The temperature dependences of the viscosity for molten CuBr and CuI.

6. Discussion

As seen in figures 9 to 11, the simulated diffusion constant obeys the following activation formula, although this has not been obtained theoretically for the liquid state:

$$D = D_0 \exp\left(-\frac{Q}{RT}\right) \tag{13}$$

where Q is the so-called activation energy, indicating the slopes in these figures.

Therefore the value Q is, more or less, an empirical quantity at the present stage. However, it is interesting to compare the value of Q for a positive ion and that for a negative one. The values of D_0 and Q derived from the simulated values are shown in table 3.

In the case of molten CuCl, the results agree qualitatively with those obtained from tracer experiments [23].

It is stressed that the activation energy Q for Cu^+ ions in molten CuI is very close to that for I^- ions, and this may be ascribed to the fact that the ionic configurations of the neighbouring ions for Cu^+ ions and I^- ions are nearly the same, as shown in figure 2, while the value of Q for Cu^+ ions in molten CuCl is much smaller than that for Cl^- ions because of the difference between the ionic configurations of the neighbouring ions as described in the preceding section. In the case of molten CuBr, as seen in figure 2, the difference between the ionic configurations around Cu^+ ions and Br^- ions is intermediate compared to those for molten CuI and CuCl, and consequently the difference between the values of Q is also intermediate.

Acknowledgments

The authors wish to express their thanks to Dr M Silbert, of the University of East Anglia, for his kind and useful discussion of this work.

References

[1] Revere M and Tosi M P 1986 *Rep. Prog. Phys.* **49** 1001–81
[2] Edwards F G, Howe R A, Enderby J and Page E T 1978 *J. Phys. C: Solid State Phys.* **11** 1053–7
[3] Biggin S and Enderby J E 1982 *J. Phys. C: Solid State Phys.* **15** L305–9
[4] Saito M, Omote K, Sugiyama K and Waseda Y 1997 *J. Phys. Soc. Japan* **66** 633–40
[5] Page D I and Mika K 1971 *J. Phys. C: Solid State Phys.* **4** 3034–44
[6] Eisenberg S, Jal J F, Dupuy J, Chieux P and Knoll W 1982 *Phil. Mag.* A **46** 195–209
[7] Powles J G 1975 *J. Phys. C: Solid State Phys.* **8** 895–906
[8] Gillan M J 1976 *J. Phys. C: Solid State Phys.* **9** 2261–71
[9] Boyce J B and Mikkelsen J C Jr 1977 *J. Phys. C: Solid State Phys.* **10** L41–3
[10] See, for example,
March N H and Tosi M P 1984 *Coulomb Liquids* (London: Academic)
[11] Stafford A J, Silbert M, Trullàs J and Giró A 1990 *J. Phys.: Condens. Matter* **2** 6631–41
[12] Tosi M P and Fumi F G 1964 *J. Phys. Chem. Solids* **25** 45–52
[13] Vashishta P and Rahman A 1978 *Phys. Rev. Lett.* **40** 1337–40
[14] Inui M, Takeda S and Uechi T 1991 *J. Phys. Soc. Japan* **60** 3190–1
[15] *CRC Handbook of Chemistry and Physics* 1987 ed R C Weast (New York: Chemical Rubber Company Press)
[16] Verlet L 1967 *Phys. Rev.* **159** 98–103
[17] Lees W and Edwards S F 1972 *J. Phys. C: Solid State Phys.* **5** 1921–9
[18] Levesque D, Verlet L and Kürkijarvi J 1973 *Phys. Rev.* A **7** 1690–9
[19] Ashurst W T and Hoover W D 1974 *Phys. Rev.* A **11** 658–78
[20] Allen M P and Tildesley D J 1987 *Computer Simulation of Liquids* (Oxford: Clarendon)
[21] Trozzi C and Ciccotti G 1984 *Phys. Rev.* A **29** 916–25
[22] Trullàs J, Giró A and Silbert M 1990 *J. Phys.: Condens. Matter* **2** 6643–50
[23] Poignet J C and Barbier M J 1981 *Electrochim. Acta* **26** 1429–34
[24] Shirakawa Y 1993 *Doctoral Dissertation* Niigata University